General Medicine: Open Access
ISSN: 2327-5146

Chu and Su, General Med 2015, 3:2
DOI: 10.4172/2327-5146.1000172

Research Article Open Access

Automated Data Collection and Analysis for Ubiquitous and Continuous Electronic Fetal Monitoring

Ta-Wei Chu[1*] **and Chuan-Jun Su**[2]

[1]*Department of Obstetrics and Gynecology, Tri-service General Hospital, National Defence Medical Center, Taipei MJ Health Screening Center, Taipei, Taiwan*

[2]*Department of Industrial Engineering & Management, Yuan Ze University 135, Far-East Rd., Chung-Li, Taiwan*

[*]**Corresponding author:** Chuan-Jun Su, Department of Industrial Engineering & Management, Yuan Ze University 135, Far-East Rd., Chung-Li, Taiwan, Tel: +81-75-465-7664; E-mail: iecjsu@saturn.yzu.edu.tw

Rec date: July 4, 2014 **Acc date:** March 19, 2015 **Pub date:** March 27, 2015

Abstract

Electronic fetal monitoring (EFM) systems have become a very promising tool over last few decades to facilitate monitoring among different practitioners, such as midwives, obstetricians, and labor and delivery nursing staff. The inception of electronic fetal monitoring systems encourages the integration of many clinical activities in fetal monitoring; however, advanced technologies have not provided obstetrician with the opportunity to promote pervasive fetal monitoring services with real time status examinations due to the lack of a means for automatic and continuous monitoring. In this paper we describe an automated EFM diagnosis tool (AEDT) that is capable of continuously and automatically collecting and analyzing the EFM data. By integrating the AEDT with light-weight, portable fetal monitor devices, continuous long-term monitoring can be performed without interfering with a patient's everyday activities and without restricting her mobility.

Keywords: Electronic fetal monitoring (EFM); Automated diagnosis; Ubiquitous and continuous electronic fetal monitoring

Introduction

Electronic fetal monitoring (EFM) is a form of fetal surveillance in labor to ensure the healthiest birth outcome. The traditional fetal monitor records an unborn baby's heart rate during pregnancy and labor and graphs it on a piece of paper. The fetal monitor is the best way to evaluate an unborn baby, and it is almost the only test to make sure that a baby's well-being during labor.

The rapidly rising Internet technologies have helped drive the growth of EFM systems in recent years. EFM systems leverage the electronic apparatus and information technology (IT) to support a variety of fetal monitoring information, technologies, and/or services. Before EFM systems were introduced in the 1950's, physicians and nurses could only periodically monitor the baby's heartbeat by listening to the heartbeat using a stethoscope and physical examination by palpitation of the female anatomy surrounding the fetus [1].

This approach was a great help for obstetricians to monitor fetal well-being. However, it is usually performed during relatively short periods of time during a visit to the physician's office.

It fails to furnish sufficient data concerning the health of the fetus in response to varying environmental conditions and catch subtle changes in lifestyle confronting the mother and fetus. In addition to the recognized risks associated with alcohol, tobacco and drug consumption, there are such environmental factors as exposure to industrial and agricultural chemicals. Activities such as running and hiking all have impact on fetal well-being.

In order to effectively monitor and warn the gravida of many health risks to the fetus, an automatic mechanism for fetal monitoring is needed. In this paper we describe our development of an automatic, interactive, and customizable methodology that can continuously and automatically analyze fetal well-being using heart rate patterns and uterine pressure parameter based upon physician's domain know-how. With the methodology, ubiquitous and continuous monitoring of fetus well-being can be realized and the difference between life and death in critical circumstances can be possibly made.

Literature Review

Intrapartum fetal asphyxia is an important cause of stillbirth and neonatal death. Some neonates with intrauterine hypoxia require resuscitation and other aggressive medical interventions for such complications as acidosis and seizures.

The principal screening technique for fetal distress and hypoxia during labor is the measurement of fetal heart rate. Abnormal decelerations in fetal heart rate and decreased beat-to-beat variability during uterine contractions are considered to be suggestive of fetal distress. Professor K. Hammacher and Hewlett-Packard, Inc. produced the first commercial harmless electronic fetal monitor (EFM) in 1968 [2]. Advances in fetal monitor development have paralleled computer and ultrasound development.

The apparatus was used to monitor the fetal heartbeat (or heart rate) and maternal uterine contractions (UC) during labor and mainly focused on showing the output of each heart cycle for discriminating between the first and second heart sounds. Fetal heartbeat data is so valuable that we need to monitor the fetal heart rate continuously and collect the recordings.

The pattern of the baby's heartbeat during labor often cannot only indicate at least some incidents of fetal distress, but can also be taken as evidence of the baby's condition. Aprecipitous drop in the heart rate after a contraction could imply animminent fetal devise if delivery is not effected immediately.

The detection ofthese patterns during monitoring by auscultation or during electronic monitoring (cardiotocography) increases the likelihood that the fetus is in distress, but the patterns are not diagnostic.

In addition, normal or equivocal heart rate patterns do not exclude the diagnosis of fetal distress [1]. Precise information on the frequency of false-negative and false-positive results is lacking, however, due in large part to the absence of an accepted definition of fetal distress [3,4].

Continuous intrapartum fetal monitoring cardiotocogram (CTG) and fetal heart rate (FHR) pattern classification is highly labor-intensive. Computerized FHR diagnosis is intended to provide accurate and simple evaluation of FHR to minimize the labor of CTG analysis and to maximize the effectiveness of fetal monitoring.

The objective is to arrive at an electronically-quantified interpretation of the FHR tracing as an aid to the subjective interpretation of the human eye. Even experts show low rates of agreement in visual interpretation of the EFM tracing [5]. A key limitation in the design of visual analysis studies has been the absence of standardized, quantified, or sometimes even identified FHR pattern definitions.

EFM devices help prevent dystocia during labor, so they are often used for routine monitoring of women in labor. Beat-to-beat variability is described quantitatively by indices originating from invasive fetal electrocardiography which provides the fetal heart rate (FHR) signal in the form of a time event series.

Thus fetal wellbeing can be significantly predicted by analyzing the FHR variability. Janusz et al. presented a method for FHR signal processing that ensures accurate extraction of the time series of events from the sampled signal by reducing FHR signal distortions related to duplicated and invalid samples [6].

Another advance made by [7] was the development of an artificial neural network based on the logical interpretation of fuzzy if-then rules for evaluating the risk of low fetal birth weight using the quantitative description of cardiotocography signals. Additional innovations in FHR detection have accelerated the advancement of EFM technology [8,9].

With the development of wireless communications technologies, portable monitoring devices can be used in the office, the clinic, and even in the home with fetal data transmitted from remote locations via telephone or modem for analysis of fetal wellbeing.

There is a similar issue as in [10]. “We need to agree on what agreement is”. Simple guidelines are still insufficient to perform the accurate and reliable diagnoses. Incorporating sophisticated diagnostic methodologies into AEDT can effectively enhance the functionality of the system.

Computer software for the FHR analysis performs objective mathematical analysis based on predetermined criteria for both antepartum testing and labor settings. There must be agreement on which FHR features are assessed, how patterns are defined, and the criteria for a reassuring tracing. The most common computerized FHR feature is baseline rate; additional features might include variability, accelerations, and decelerations.

Investigators have compared clinician visual analysis of fetal tracing to computerized mathematical analysis which provided better reliability [11]. Objective and standard criteria are necessary not only for research (to establish reliability, validity, and efficacy of the technology), but also for meaningful communication among caregivers, legally defensible documentation, and databases.

We aim to develop an automated EFM diagnosis tool (AEDT) with mathematical criteria on fetal heart beats and uterine contractions in the analysis of intrapartum surveillance, and therefore more objective results were expected than those in the past studies.

Categorization and Analysis of Fetal Heart Monitoring Records

Categorization of symptoms

In Klavan, Laver and Boscola's Clinical Concepts of Fetal Heart Rate Monitoring [1], the authors state that “before delivery it is impossible to be fully aware of a fetus at risk”. Through examination of medical records, coupled with changes in heart rate of the fetus as well as uterine contraction rate of the mother, we can discern five types of risk symptoms: tachycardia, brady cardia, early deceleration, late deceleration and variable deceleration. The characteristics of these symptoms are described as follows:

Tachycardia: Tachycardia refers to the fetal heart ratio above the average rate (saysover 160 bpm). Tachycardia occurs for a variety of reasons, but is generally not directly related to uterine contraction.

Bradycardia: Bradycardia refers to a fetal heart ratio which is too slow, below an average rate of 110 bpm. The impact of this condition on the fetus is significant; resulting in death in the most severe cases, so close monitoring is required.

Early Deceleration: Early deceleration yields a curve consistent with uterine contractions, almost without a time lag. The graph drawn by the fetal heart monitor for this symptom shows coinciding periods for the fetal heart rate and the mother's uterine contractions.

Late Deceleration: Late deceleration draws a regular curve mirroring uterine contractions, which is the opposite of early deceleration, presenting an inverted bell curve. A lag consistently occurs at the beginning, peak and end of each contraction.

Variable deceleration: Variable deceleration may, as the name suggests, be of various shapes, including a U shape, V shape and unrelated to uterine contractions. This condition presents the most commonly observed risk symptom, observed in 80% of birth delivery procedures. Some irregular deceleration is not even related to uterine contractions, but rather related to movement of the fetus.

Analysis of symptoms

The characteristics of five major symptoms of fetal heart rate monitoring suggested above provide mostly a qualitative description of the symptoms. Therefore, the accuracy of diagnosis results highly relies on the experience of obstetricians. To reduce the potential human error and to extend the application to the use of automatic devices, the development of quantitative rules will be needed. Before start to process the data collected, we discussed the diagnosis procedure of case histories with the obstetrician and establish the rules for five symptoms, respectively.

Since each doctor may have different opinions at diagnosis, the quantitative rules we formulated are not intended to completely match the standards of each doctor. These rules do not diverge greatly, however, so during actual operations, only minor adjustments to rule

parameters are required to meet the diagnostic requirements of diverse doctors.

The diagnosis rules of five symptoms are as follows. Each symptom will be discussed with an illustrative example, and the details of the rules will be defined consequently. Before introducing the rules, proper definition of notations are shown below (Figures 1-5).

HR_s: The start time of a heart rate change cycle.

HR_e: The end time of a heart rate change cycle.

HR_P: The point of nadir in a heart rate change cycle.

UC_s: The start time of a uterine contraction cycle.

UC_e: The end time of a uterine contraction cycle.

UC_p: The point of peak in a uterine contraction cycle.

HS_p: The point of peak in a heart rate acceleration cycle (called a shoulder region and appeared in Variable Deceleration only).

HS_e: The end time of a heart rate accelerationcycle (called a shoulder region and appeared in Variable Deceleration only).

B: The heart rate of a baseline.

Tachycardia

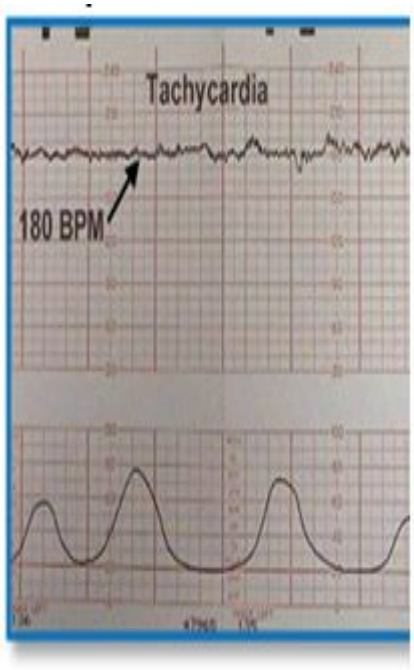

Figure 1: An example of Tachycardia, a. The heartbeat ratio160 bpm b. The period of the condition above must last at least three minutes

Bradycardia

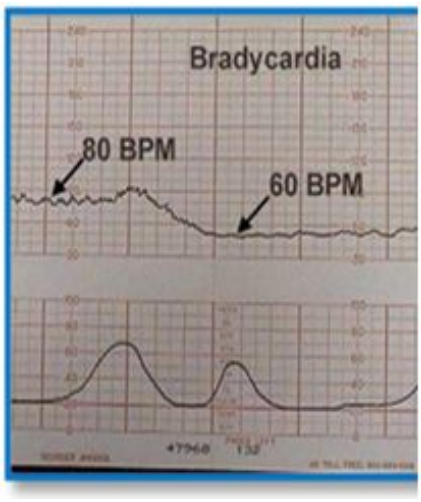

Figure 2: An example of Bradycardiaa, The heartbeat ratio10 bpm b. The period of the condition above must last at least three minutes.

Early Deceleration

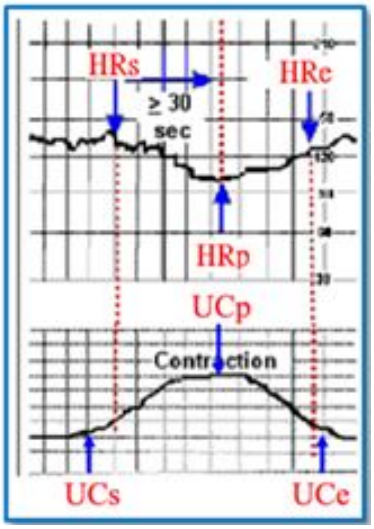

Figure 3: An example of Early Deceleration, a. $HR_p<UC_e$, i.e. the heart rate reaches its nadir before the uterine contraction cycle completes. b. $HR_p–HR_s$ 30, i.e. the lag between the point the heart rate begins to drop and the point reaches its nadir is over 30 seconds. c. HR_sUC_s+5, i.e. the lag between the point when the heart rate begins to drop and the point when the uterine contraction begins must be over five seconds. d. $B–HR_p$ 15, i.e. the nadir of a heart rate change cycle must be at least 15 beats below the baseline.

Late Deceleration

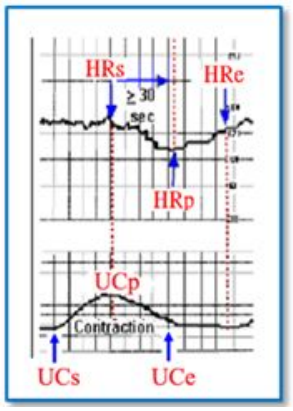

Figure 4: An illustration of Late Deceleration, a. HR_pUC_e, i.e. the heart rate change cycle does not reach its nadir until after the completion of a uterine contraction. b. HR_p–HR_s 30, i.e. the lag between the point the heart rate begins to drop and its nadir is over 30 seconds. c. B–HR_p 15, i.e. the nadir of the heart rate change cycle must be at least 15 beats below the baseline.

Variable Deceleration

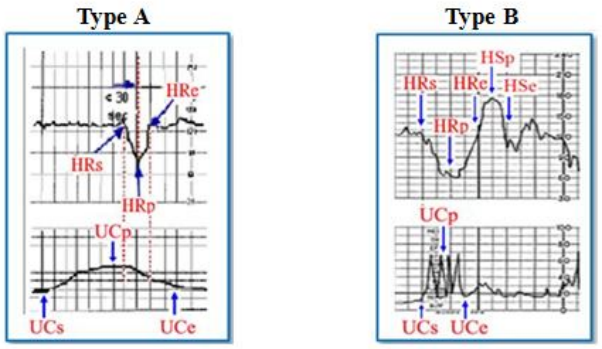

Figure 5: Examples of Variable Deceleration (type A and type B). **Type A:** a. HR_p – HR_s 30, i.e. the lag between the point the heart rate begins to drop and the point reaches its nadir is no more than 30 seconds. b. HR_sUC_s+5, i.e. the point that the heart rate begins to drop must be over five seconds later than the beginning of the uterine contraction. c. B–HR_p 15, i.e. the nadir of the heart rate change cycle must be at least 15 beats below the baseline. **Type b:** a. HR_s UC_s+5, i.e. the point that the heart rate begins to drop must be over five seconds later than the beginning of the uterine contraction. b. B–HR_p 15, i.e. the nadir of the heart rate change cycle must be at least 15 beats below the baseline. c. HS_p–B 10, i.e. the peak of shoulders of acceleration after deceleration must be at least 10 beats above the baseline. d. HS_e–HR_e 10, i.e. The lag of shoulders of acceleration must last at least 10 seconds

Data Processing

Data collection and pre-processing

Since the machines and equipment of different hospitals vary, data collected over the course of the research period was in both digital and traditional paper graph form. If the data was in digital format, it could be directly entered into the diagnostic program to perform symptom diagnosis. Graph printouts, on the other hand, had to be preprocessed into a digital format before it could be entered into the program for processing. The digitization procedure of graph printouts is summarized as follows:

A scanner was used to convert the record printout into a digital image.

Corel PhotoImpact® was used to cut the digital image into appropriate sizes, and to remove unneeded text from the image which could contribute to misinterpretation.

The image is read into the program, and then the baseline and peak (minimum and maximum) of heart rate change cycle and contraction cycle are identified.

Microsoft Excel® is used to generate a curve from the set of digital data points which is then compared to the original image of the paper graph to validate data correctness and precision.

Several issues arise when the paper-based data is digitized. First of all, when doctors use graph printouts for their diagnostics, they write notes on the printout, which causes problems when removing noise. For example, a doctor may circle a problem area in the graph to make a note of it. Then, when the software program detects darker markings on the paper to digitize the graph, care must be taken to remove noise (including the handwriting) from the data; otherwise human factors may lead to poor results.

Secondly, the graph printout is composed of dots so there are missing dots over the course of larger variations. Thus, we used the interpolation method to connect truncated data [12]. For example, in the original medical charts as shown in Figure 6, we can see the manifestation of symptoms circled in red, while the areas circled in blue are uncertain areas of the graphs, requiring the application of interpolation for further interpretation. Bringing the data into Microsoft Excel® as illustrated in Figure 7, the curves of the contraction and the corresponding heart rate change cycle can be identified more clearly. However, this technique has to be applied with caution because it may impact the results of curve fitting, resulting in serious skewing of the diagnostic points and leading in turn to inaccurate diagnosis of the symptoms.

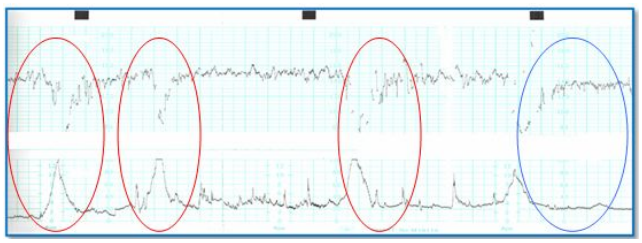

Figure 6: The scanned original monitoring output

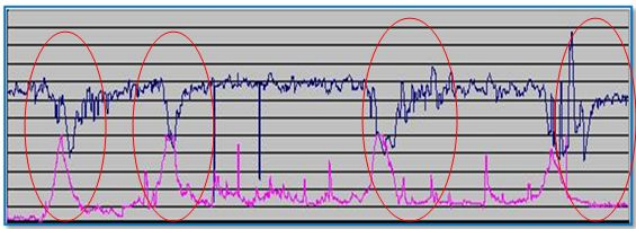

Figure 7: The graph after adding points generated by interpolation in Excel

Lastly, from the interview with obstetricians, we realized that the doctor requires an interval of eight to ten minutes to interpret the output graph. Note that the monitoring equipment records two points per second, and the fetus's heart beats also twice per second on average. To increase the overall accuracy of symptom detection, and take into account issues with equipment of the Armed Forces Hospital, we decided to divide the original data into 1000-point segments to accommodate the time required for the doctor to interpret the graph. However, since it would be difficult to determine where the segments are separated properly, the overlapped segments are employed. That is 50% of points will be overlapped in two consecutive segments as illustrated in Figure 8.

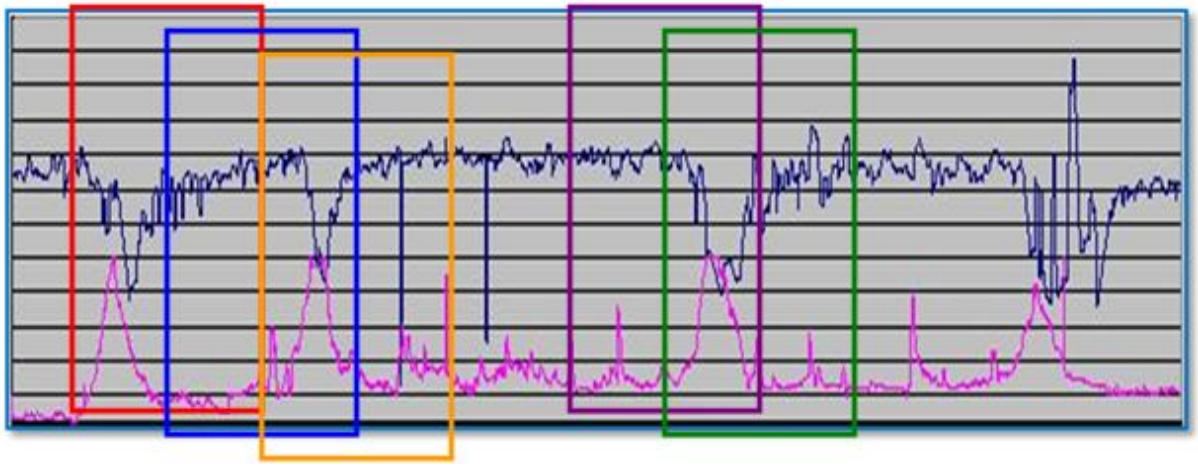

Figure 8: An illustration of segmentation for the graph after adding points generated by interpolation in Excel

Data smoothing

As we know, cases vary from patient to patient, so a significant amount of randomness is present in the data of this study. Therefore, after the paper record is transformed to the digital data, we apply the conventional moving average method to smooth out the noise and address randomness in the data (13-15).

A simple moving average method sums up the values collected in recent k periods, and find the average value to estimate the value of the k+1 period. If the value of the i^{th} period is denoted as y_i, then the estimated value for period k+1 (denoted by F_{k+1}) can be represented by the following formula:

$$F_{k+1} = \frac{y1+y2+\cdots+yk-1+yk}{k}$$

The main features in the moving average method consist of a) each observed value is assigned the same weight, b) the same number of data points is used for each calculation. An illustration of a data set after applying the smoothing technique is shown in Figure 9. In addition, all operations in data smoothing, curve fitting, and symptom diagnosis thereafter are all performed using MATLAB®.

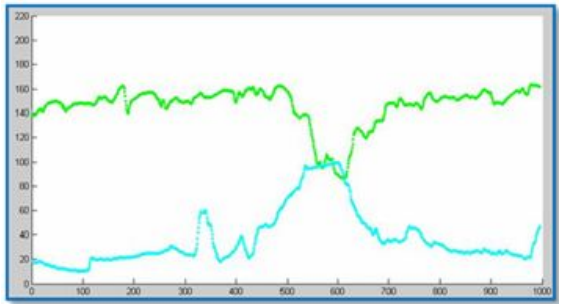

Figure 9: An example of smoothed image

Curve fitting

Since the digital data are obtained thru the scanning step from paper output, interpolation of the missing points, and the smoothing procedure, it is easy to introduce errors that cause the loss of originality of data. In the preliminary study, various curve fitting methods were applied to the smoothed data to discover the best curve fitting equation which leads to the Gaussian function as follows [16-18].

$$y = \sum_{i=1}^{n} a_i e^{\left[-\left(\frac{x_i - b_i}{c_i}\right)^2\right]}$$

Whereai, *bi*, and *ci* denote mean, standard deviation, and coefficient parameters in the Gaussian function, respectively. n represents the number of Gaussian functions adopted in the model. Therefore, the kernel of Gaussian functions consists of the linear summation of several Gaussian functions. Figure 10 illustrates an outcome of curve fitting by the Gaussian kernel.

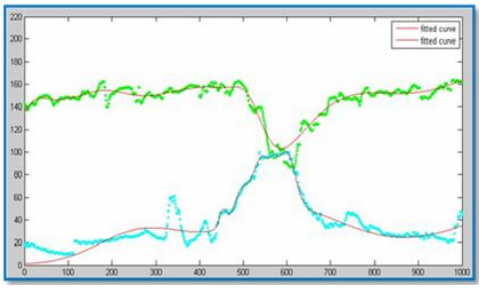

Figure 10: An illustration of curve fitting with a Gaussian kernel

Case Study and Discussion

This section will start from an illustrative example of the symptom diagnosis procedure proposed in this study, and then we will apply the procedure to a data set with 20 patients with known outcomes for the case study.

Illustrations of symptom diagnosis procedure

The symptom diagnosis procedure starts once all the data acquisition and processing (including digitalization, smoothing, and curve fitting) process have been completed. Because of the irregular ups and downs of fetal heart beats, obstetricians indicate actual problems in fetal heart rate when they are affected by uterine contractions. So to diagnose the pathological findings we must obtain the data points we actually need. We obtain the uterine contraction peak (UC_p) from a point higher than its two adjacent points, and from the peak move down to find the intersection with the baseline, which we set as the starting (UC_s) and ending point (UC_e) of the contraction.

We then relate the beginning point of the uterine contraction with the fetal heart beat data. Thereafter we search for the nearest start (HR_s) in drop of heart beat rate, the nadir (HRP) and the end (HR_e) of the drop in heart rate.

Then, we apply the pathological definitions previously agreed upon with the obstetrician (as defined in Section, Analysis of Symptoms) to complete the diagnosis. We will describe the procedure of key point's extraction by an illustrative example as in Figure 11. The green curve represents the heart rate and the blue curve denotes the uterine contraction. In addition, two fitted curves are plotted using the red color, respectively.

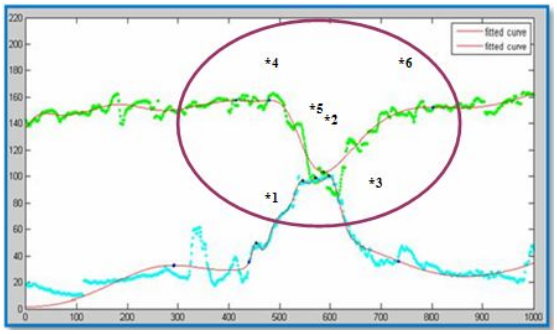

Figure 11: An example of case analysis

Since the peak and nadir of the uterine contraction are more regular than the heartbeat, we start the key points extraction procedure from the beginning of the contraction cycle (point *1 in Figure 11) and move forward from there, looking for the peak of the heart rate (point *4). From here the heart rate begins to drop. Again, back to the curve of the uterine contraction, we move forward searching for the contraction peak (point *2), and then to the end of the contraction cycle (point *3). Starting from the point (point *4) that the heart rate begins to fall, we move forward looking for the nadir (point *5), and the point where the heart rate stops dropping (point *6), i.e. back to the baseline level. In this way we collected all the key points required by the diagnostic procedure, and then, we can apply the rules developed in Section 3.2 to judge whether or not there are any symptoms of abnormalities. The following is the discussion for each rule.

Tachycardia: The heart rate in Figure 11 is always lower than 160 bpm, so we can easily conclude that this case is not Tachycardia since it cannot satisfy the first criterion, i.e. the heart beat ratio160 bpm.

Bradycardia: The heart rate in Figure 11 does fall below 110 bpm for a certain period of time. However, it lasts for only about 20 seconds which is much shorter than the requirement in the second criterion for Bradycardia, i.e. the heart rate lower than 110 bpm lasts for at least three minutes. Thus, we can conclude that this case does not belong to the symptom of Bradycardia either.

Early deceleration: In Figure 11, the fetal heart rate reaches its nadir before the contraction completes, i.e. agreeableon rule 1: $HR_p < UC_e$. Since the equipment is set to plot a point twice every second, the distance between the nadir heart rate and the beginning of the fall of heart rate is approximately 90 points, so we assume that the time between when the heart rate began to fall and reached nadir is 45 seconds which satisfies rule 2: $HR_p - HR_s$ 30. The interval between the beginning of the drop in fetal heart rate and the beginning of uterine contraction is over 10 points, meaning that the uterine contraction had already begun for more than five seconds when the heart rate began to fall (rule 3: HR_s UC_s + 5). Lastly, the greatest difference between the baseline and the point of nadir fetal heart rate is approximately 45 beats which also fulfills the requirement of rule 4: B – HR_p 15. Based on the results above, we can be certain that this is a case of early deceleration.

Late deceleration: From Figure 11, we can see that the nadir of fetal heart rate occurred before the completion of uterine contraction

(violation of rule 1: HR_p UC_e), so we can be sure this is not a case of late deceleration.

Variable deceleration type A

In the graph of Figure 11, the heart rate took over thirty seconds from the beginning of rate decrease until it reached nadir, so it is against rule 1: HR_p – HR_s 30. Therefore, we can be sure this is not a case of Type A variable deceleration.

Variable deceleration type B

As observed from Figure 11, the interval between the beginning of the drop in fetal heart rate and the beginning of uterine contraction is over 10 points, meaning that the uterine contraction had already begun for more than five seconds when the heart rate began to fall. This leads to the satisfaction of rule 1: HR_s UC_s + 5.Secondly, the greatest difference between the baseline and the point of nadir fetal heart rate is approximately 45 beats which also fulfills the requirement of rule 2: B – HR_p 15.However, no shoulder region can be found in the heart beat change cycle, so we can be sure this is not a case of Type B variable deceleration.

From the diagnosis procedure above, we have successfully identified a symptom of early deceleration, and then doctors can prescribe further medical treatments if necessary.

Case study

This section will conduct a case study based on the proposed diagnosis procedure. The data was collected from the Taoyuan Armed Forces General Hospital, Lung-Tan, Taiwan. The medical records consist of 20 patients and were divided into 211 figures (i.e. cases) with the equal window size as described in Section, Data Collection and Pre-processing. Table 2 summarizes the symptoms categorized by the obstetricians, 66 abnormal symptoms out of 211 figures are identified. Table 3 compares the results by our diagnosis procedure with the observations by the obstetricians. It is clear that our procedure can obtain 98.5% detection rate and 92.4% of diagnosis accuracy. Only five cases were misdiagnosed (four of them were diagnosed as different symptoms, and one abnormal case was classified as a normal one).

When applying National Institute of Child Health and Human Development (NICHD) Guidelines on Fetal Heart Rate Monitoring from a sample of 20 women, our data indicated a positive predictive value of 92.4 % for AEDT and to obstetrics. Diagnosed pattern error is due to poor data quality (signal loss or noises).As we can see from Table 3, we misdiagnosed early deceleration as late deceleration in three cases while we misidentified another early deceleration case as the normal condition. Part of the reason for interpretation errors is the high similarity of graphs for early deceleration and late deceleration. However in overall interpretation, late deceleration is more important and more serious than early deceleration. Even though interpretation of this part of the case diverges from the opinion of doctors, we may still consider it as an effective diagnosis. Meanwhile the reason for the undiagnosed case is that the case graph does not accommodate the rules we derived with the doctors, but when strictly judged from the doctor's experience, the case can be diagnosed as early deceleration. After discussing it with the doctors, they decided to treat the case as a special case, which we leave for future discussion.

Patterns	Normal	Early deceleration	Late deceleration	Variable Deceleration	Tachycardia	Bradycardia
Quantity	145	16	20	11	17	2

Table 1: Summary of symptoms on 211 graphs.

Patient	Doctor's Diagnosis	Diagnosis of the Procedure			Notes
	(Abnormal Symptoms)	Correct Diagnosis	Incorrect Diagnosis	Not Diagnosed	
A	0	0	0	0	Diagnosed as normal
B	1	1	0	0	Diagnosed as early deceleration
C	4	3	1	0	Diagnosed as tachycardia
D	4	4	0	0	Diagnosed as early deceleration
E	4	4	0	0	Diagnosed as early deceleration and variable deceleration type A at the late stage
F	1	1	0	0	Diagnosed as late deceleration
G	4	4	0	0	Diagnosed as late deceleration
H	6	6	0	0	Diagnosed as tachycardia
I	3	2	1	0	Our procedure diagnosed as late deceleration, but one of the symptoms diagnosed as early deceleration by the obstetrician

J	2	2	0	0	Diagnosed as variable deceleration type A
K	2	2	0	0	Diagnosed as brady cardia
L	21	19	2	0	Our procedure diagnosed as variable deceleration type A combined with the symptom of late deceleration, but the obstetrician diagnosed the late deceleration as the early deceleration
M	0	0	0	0	Diagnosed as normal condition
N	1	1	0	0	Diagnosed as tachycardia
O	1	0	0	1	Our procedure diagnosed as the normal case, but the obstetrician diagnosed as early deceleration
P	2	2	0	0	Diagnosed as late deceleration
Q	4	4	0	0	Diagnosed as tachycardia with aspects of late deceleration
R	4	4	0	0	Diagnosed as tachycardia
S	1	0	0	0	Diagnosed as late deceleration
T	1	1	0	0	Diagnosed as early deceleration
Total	66	61	4	1	

Table 2: Comparison of diagnosis results between the obstetricians and the proposed procedure.

After discussing with obstetricians, some reasons for discrepancies in this study are categorized as follows:

1. Unclear original graph: Interpolation is used to fill in missing points resulting from breaks and gaps in the data caused by the scanning of the original images or from other reasons. This impacts the result of curve fitting, which further impacts the selection of key points.
2. Inconsistency between the image and the original case graph: Inconsistencies were found between the graphs plotted using MATLAB® and the original case graphs. As the MATLAB® graph is larger than the original graph and because doctors make decisions as quickly as possible based on their own experience, inconsistencies between the graphs may result in doctors misjudgement when making diagnoses.
3. Errors in extracting key points: The current criteria for selecting key points is to first find the maximum and minimum points, then look for the first drop affected by contraction following the first contraction. Sometimes the first drop in heart rate after a contraction is a mild one, and the following ups and downs are more pronounced. For the doctor, the more prominent rises and falls are the interesting data, which can also result in mismatched diagnosis.

References

1. Klavan M, Laver AT, Boscola MA (1980) Clinical Concepts of Fetal Heart Rate Monitoring.
2. Dawson A, Cohen D, Candelier C, Jones G, Sanders J, et al. (1999) Domiciliary midwifery support in high-risk pregnancy incorporating telephonic fetal heart rate monitoring: A health technology randomized assessment. J. Telemed. Telecare 5: 220–230.
3. Goodlin RC, Haesslein HC (1977) When is it fetal distress? Am J Obstet Gynecol 128: 440–445.
4. Prentice A, Lind T (1987) Fetal heart rate monitoring during labour: too frequent intervention, too little benefit? Lancet 2: 1375–1377.
5. American College of Obstetricians and Gynecologists Committee on Obstetric Practice. Fetal distress and birth asphyxia (1994) Committee Opinion no. 137. Washington, DC: American College of Obstetricians and Gynecologists.
6. McCartney P (2004) Leadership in nursing informatics. Journal of Obstetric, Gynecologic and Neonatal Nursing 33: 371-380.
7. Jezewski J, Kupka T, Horoba K (2008) Extraction of fetal heart-rate signal as the time event series from evenly sampled data acquired using doppler ultrasound technique. IEEE Trans. Biomed. Eng 55: 805–810.
8. Czabanski R, Jezewski M, Wrobel J, Jezewski J, Horoba K (2010) Predicting the risk of low-fetal birth weight from cardiotocographic signals using ANBLIR system with deterministic annealing and bm ε-insensitive learning. IEEE Trans. Inf. Technol. Biomed. 14: 1062–1074.
9. Karvounis EC, Tsipouras MG, Fotiadis DI (2009) Detection of fetal heart rate through 3-D phase space analysis from multivariate abdominal recordings. IEEE Trans. Biomed. Eng 56: 1394–1406.
10. Sahin I, Yilmazer N, Simaan MA (2010) A method for subsample fetal heart rate estimation under noisy conditions. IEEE Trans. Biomed. Eng 57: 875–883.
11. Costa-Santos C, Ayres-de-Campos D, Bernardes J (2011) Comparison of experts and computer analysis in fetal heart rate interpretation: we need to agree on what agreement is. Am J Obstet Gynecol. 204: e11-12
12. Carroll RJ, Ruppert D (1988) Transformations and Weighting in Regression, Chapman & Hall, London.
13. Cleveland WS (1979) "Robust Locally Weighted Regression and Smoothing Scatterplots," Journal of the American Statistical Association 74: 829-836.
14. Goodall C (1990) "A Survey of Smoothing Techniques," Modern Methods of Data Analysis, (Fox J and Long JS (eds.)), Sage Publications, Newbury Park, CA 126-176.
15. Bevington PR, Robinson DK (1992) Data Reduction and Error Analysis for the Physical Sciences, 2nd Ed., WCB/McGraw-Hill, Boston.

16. Cleveland WS, Devlin SJ (1988) "Locally Weighted Regression: An Approach to Regression Analysis by Local Fitting," Journal of the American Statistical Association 83: 596-610.

17. De Boor C (1978) A Practical Guide to Splines, Springer-Verlag, Berlin.

18. MATLAB: Curve fitting Toolbox User's Guide, The MathWorks, Inc., 2007.